STOKES DRIFT ESTIMATION FOR DEEP WATER WAVES BASED ON SHORT-TERM VARIATION OF WAVE CONDITIONS

Dag Myrhaug[1], Hong Wang, Lars Erik Holmedal

Department of Marine Technology
Norwegian University of Science and Technology (NTNU)
NO-7491 Trondheim, Norway
[1]E-mail: dag.myrhaug@ntnu.no

ABSTRACT

The paper provides a simple analytical method which can be used to give estimates of the Stokes drift based on short-term variation of wave conditions. This is achieved by providing bivariate distributions of wave height and surface Stokes drift as well as wave height and volume Stokes transport for individual random waves within a sea state. The paper presents and discusses statistical aspects of these Stokes drift parameters, as well as examples of results corresponding to typical field conditions.

Keywords: Surface gravity waves; Stokes drift; Wave height; Individual waves; Bivariate distributions.

1. INTRODUCTION

The Stokes drift represents an important transport component in the ocean. Locally it is responsible for transport of e.g. contaminated ballast water from ships, oil spills, plankton, larvae. It is also involved in mixing processes across the interphase between the atmosphere and the ocean. The Stokes drift is obtained as the mean Lagrangian velocity yielding the water particle drift in the wave propagation direction, with its maximum at the surface and decreasing with the depth below the surface. The total mean mass transport is obtained by integrating the Stokes drift over the water depth; also referred to as the volume Stokes transport by Rascle et al. (2008). More details of the Stokes drift are given in e.g. Dean and Dalrymple (1984).

The Stokes drift and the volume Stokes transport were originally defined for regular waves. However, their characteristic quantities for random waves in terms of the sea state parameters significant wave height and characteristic wave periods are also defined (see e.g. Rascle et al. (2008); Webb and Fox-Kemper (2011)). A global data base for parameters associated with ocean surface mixing and drift including the surface Stokes drift and the volume Stokes transport among other parameters by performing wave hindcast of the wave parameters was described by Rascle et al. (2008). The hindcast results of Rascle et al. (2008) was improved by Rascle and Ardhuin (2013) using new parameterizations of the physical processes involved (see their (2013) paper and the references therein for more details). Relationships between the wave spectral moments and the Stokes drift in deep water at an arbitrary elevation in the water column were considered by Webb and Fox-Kemper (2011), and inter-comparisons were made using different spectral formulations. Myrhaug (2013, in press) presented bivariate distributions of significant wave height with surface Stokes drift and volume Stokes transport. Myrhaug (2013) also presented bivariate distributions of spectral peak period with these two Stokes drift parameters. Based on this some statistical aspects of the

Stokes drift parameters together with example of results corresponding to typical field conditions were presented.

The purpose of this study is to give a simple analytical method which can be used to estimate the Stokes drift for individual random waves based on short-term variation of wave conditions available in e.g. joint distributions of wave height (H) and wave period (T). This is obtained from parametric models of a joint distribution of wave height and surface Stokes drift as well as a joint distribution of wave height and volume Stokes transport. This is achieved by transformations of the joint distribution of H and T proposed by Longuet-Higgins (1983). Examples of calculating the mean values of the surface Stokes drift and volume Stokes transport within a given sea state corresponding to typical field conditions are also provided to demonstrate the application of the method. Thus, the present results can be used to estimate the Stokes drift for random waves within a sea state based on available wave statistics.

2. THEORETICAL BACKGROUND

Following Dean and Dalrymple (1984) the mean (time-averaged) Lagrangian mass transport at an elevation z_1 in the water column in finite water depth h is given as

$$\bar{u}_L = \frac{ga^2k^2}{\omega}\frac{\cosh 2k(z_1+h)}{\sinh 2kh} \qquad (1)$$

Here, g is the acceleration due to gravity, a is the linear wave amplitude, k is the wave number corresponding to the cyclic wave frequency ω given by the dispersion relationship $\omega^2 = gk\tanh kh$. Eq. (1) indicates that the water particles drift in the wave propagation direction; this drift has its maximum at the mean free surface $z_1 = 0$ and decreases towards the bottom as $z_1 \to -h$. In deep water Eq. (1) reduces to

$$\bar{u}_L = \frac{ga^2k^2}{\omega}e^{2kz_1} \quad ; \quad \omega^2 = gk \qquad (2)$$

The Lagrangian mass transport is often referred to as Stokes drift.

The total mean (time- and depth-averaged) mass transport, i.e. obtained by integrating Eq. (1) over the water depth, is given as (Dean and Dalrymple, 1984)

$$M = \frac{\rho g a^2 k}{2\omega} \tag{3}$$

where ρ is the density of the fluid. M is often referred to as the Stokes transport. More details of the Stokes drift and the Stokes transport are given in Dean and Dalrymple (1984).

In deep water (i.e. for large values of kh and $\omega^2 = gk$) and by substituting $a = H/2$, $\omega = 2\pi / T$, the surface Stokes drift velocity ($z_1 = 0$) in Eq. (1) can be written as

$$U_s = \frac{2\pi^3}{g}\frac{H^2}{T^3} \tag{4}$$

In a sea state of random waves Eq. (4) can be taken to represent the surface Stokes drift associated with a single random wave with wave height H and wave period T. Similarly, in deep water the total mean mass transport in Eq. (3) (also referred to as the volume Stokes transport) can be written as

$$M = \rho \frac{\pi}{4}\frac{H^2}{T} \tag{5}$$

In a sea state of random waves Eqs. (4) and (5) can be taken to represent the surface Stokes drift and the volume Stokes transport, respectively, associated with a single random wave with wave height H and wave period T.

Different models of the joint probability density function (*pdf*) of H and T are given in the literature. Examples are Cavanié et al. (1976), Lindgren and Rychlik (1982), Longuet-Higgins (1983), Myrhaug and Kjeldsen (1984), Stansell et al. (2004). Comparisons of distributions with observed wave data have been presented by e.g. Srokosz and Challenor (1987), Myrhaug and Kvålsvold (1995).

In the present paper the Longuet-Higgins (1983) (hereafter referred to as LH83) joint *pdf* of H and T is chosen to serve the purpose of demonstrating how a joint *pdf* of H and T can be used to provide statistics of U_s and M in a sea state of random waves. LH83 was derived by considering the statistics of the wave envelope, that is, the joint distribution of the envelope amplitude and the time derivative of the envelope phase. This distribution is also based on a narrow-band approximation. The LH83 joint *pdf* of wave height and wave period is given as

$$p(h,t) = C(\frac{h}{t})^2 \exp\left\{-h^2[1+\frac{1}{\nu^2}(1-\frac{1}{t})^2]\right\} \tag{6}$$

where

$$h = \frac{H}{2\sqrt{2m_0}} \tag{7}$$

$$t = \frac{T}{2\pi \frac{m_0}{m_1}} \tag{8}$$

are the dimensionless wave height and wave period, respectively, and

$$C = \frac{4}{\sqrt{\pi}\nu[1+(1+\nu^2)^{-1/2}]} \tag{9}$$

$$\nu^2 = \frac{m_0 m_2}{m_1^2} - 1 \tag{10}$$

Here m_n is the spectral moments defined as

$$m_n = \int_0^\infty \omega^n S(\omega) d\omega\,; \quad n = 0, 1, 2, ----- \tag{11}$$

where $S(\omega)$ is the single-sided wave spectrum, and ω is the circular wave frequency. The parameter ν represents a measure of the bandwidth of the wave spectrum, which may be considered narrow-band if ν is small.

LH83 presented also the marginal *pdf* of h, $p(h)$, and the conditional *pdf* of t given h, $p(t\,|\,h)$, given by, respectively

$$p(h) = Cv\frac{\sqrt{\pi}}{2}he^{-h^2}(1+erf(\frac{h}{v})) \quad (12)$$

$$p(t\,|\,h) = \frac{2}{\sqrt{\pi}v(1+erf(h/v))}\frac{h}{t^2}\exp\left[-\frac{h^2}{v^2}(1-\frac{1}{t})^2\right] \quad (13)$$

where $erf(x)$ is the error function defined by

$$erf(x) = \frac{2}{\sqrt{\pi}}\int_0^x e^{-t^2}dt \quad (14)$$

Since the spectral moments m_n are constants for each sea state, the *pdfs* in Eqs. (6), (12) and (13) are conditional *pdfs* given in a sea state, i.e. given m_n (or equivalently $S(\omega)$). It should be noted that for a narrow-band process (i.e. $v = 0$), Eq. (12) reduces to a Rayleigh *pdf*: $p(h) = 2h\exp(-h^2)$. More details about this joint *pdf* of h and t as v approaches zero are given in LH83.

By introducing the non-dimensional surface Stokes drift velocity $u = U_s / U_{char}$, Eq. (4) can be re-arranged to

$$u = \frac{h^2}{t^3} \quad (15)$$

where

$$U_{char} = \frac{2m_1^3}{gm_0^2} \quad (16)$$

is a characteristic surface Stokes drift for the sea state. Similarly, by introducing the non-dimensional Stokes transport $m = M / M_{char}$, Eq. (5) can be re-arranged to

$$m = \frac{h^2}{t} \quad (17)$$

where

$$M_{char} = \rho m_1 \quad (18)$$

is a characteristic Stokes transport for the sea state.

It should be noted that the present approach is based on assuming that the wave-induced drift (i.e. the surface Stokes drift and the volume Stokes transport) for regular waves are valid for irregular waves. This implies that each wave is treated individually, and consequently that the wave-induced drift is taken as constant for a given wave situation and that memory effects are neglected. As a result the statistical properties of the wave-induced drift in a sea state of irregular waves can be calculated by assigning to each individual wave the wave-induced drift of a regular wave with wave height H and wave period T. This assumption, often referred to as the hypothesis of equivalency, has previously been applied e.g. in calculating: (1) run-up of irregular waves on slopes (see e.g. Losada and Giminez-Curto (1981) and in the references therein); (2) bottom friction beneath random waves (Myrhaug et al. (2004), Myrhaug and Holmedal (2005)); (3) random wave-induced scour around pipelines and vertical piles (Myrhaug et al., 2009). As referred to in Losada and Giminez-Curto (1981) the hypothesis of equivalency has been verified for run-up against model test data as well as field data. For bottom friction the assumption of treating each wave individually has been justified by comparing Monte Carlo simulations and (k - ε) model predictions under irregular waves for rough turbulent flow (Myrhaug et al., 2004), and by comparing measured and simulated bed shear stresses beneath irregular waves for laminar and smooth turbulent flow (Myrhaug and Holmedal, 2005). For random wave-induced scour around pipelines and vertical piles for combined random waves and current favourable comparisons have been made between predictions and model test data. To the present authors′ knowledge no experimental data, simulations or predictions for wave-induced drift are available in the open literature for verifying the hypothesis of equivalency. Meanwhile, this hypothesis is applied as a first approximation to deduce results, which should be useful for making assessment of wave-induced drift in random waves.

3. SURFACE STOKES DRIFT

Statistical properties of the non-dimensional surface Stokes drift u (from which the statistical properties of the surface Stokes drift U_s can be obtained) can be derived by using the LH83 *pdfs* in Eqs. (6) and (13). First, the joint *pdf* of u and h is obtained from Eq. (6) by a change of variables from (h,t) to (h,u). This transformation only affects t versus u, i.e. $t = h^{2/3}u^{-1/3}$ according to Eq. (5), yielding the Jacobian $|\partial t/\partial u| = h^{2/3}u^{-4/3}/3$; corresponding to a one-to-one transformation since t decreases monotonically as u increases. Consequently the result is

$$p(h,u) = C \cdot \frac{1}{3}\left(\frac{h^2}{u}\right)^{2/3} \cdot \exp\left\{-h^2\left[1+\frac{1}{\nu^2}\left(1-\left(\frac{u}{h^2}\right)^{1/3}\right)^2\right]\right\} \tag{19}$$

Similarly, the conditional *pdf* of u given h is obtained from Eq. (13) by a change of variables from (h,t) to (h,u), yielding (by using the Jacobian $|\partial t/\partial u|$)

$$p(u\,|\,h) = \frac{2}{3\sqrt{\pi}\nu(1+erf(h/\nu))}\left(\frac{h}{u^2}\right)^{1/3}\exp\left[-\frac{h^2}{\nu^2}\left(1-\left(\frac{u}{h^2}\right)^{1/3}\right)^2\right] \tag{20}$$

It should be noted that the Jacobian is zero for $h = 0$ and has a singularity for $u = 0$. However, this does not affect the *pdfs* in Eqs. (16) and (20) as they are well defined.

Fig. 1 shows the isocontours of $p(h,u)$ for $\nu = 0.354$ (i.e. corresponding to the example given in Section 5), and the quadratic increase of u with h (Eq. 15) is clearly seen for the higher values of h. From Eq. (19) it appears that the distribution has a singularity in $h = 0$, $u = 0$.

Fig. 2 shows the *pdf* of u for $\nu = 0.1$ to 0.6 in intervals of 0.1, and is based on integration of the joint *pdf* in Eq. (19) (and in Fig. 1), reflecting that $p(u)$ has a singularity in $u = 0$. It appears that the *pdf* of u is not very sensitive to these values of ν. It should be noted that LH83 presented his joint *pdf* of h and t for these ν values.

Fig. 3 shows the expected value of u given h for $\nu = 0.1$ to 0.6 in intervals of 0.1

$$E[u \mid h] = \int_0^\infty u\, p(u \mid h) du \tag{21}$$

where $p(u \mid h)$ is given in Eq. (20). These results reflect also the feature of $p(h,u)$ in Fig. 1; $E[u \mid h]$ decreases rapidly as h increases for lower h values reaching a minimum and then it increases as h increases; the results are most sensitive to ν for the lower h values. The increase of $E[u \mid h]$ as h decreases for small h reflects the features of the LH83 joint *pdf* of h and t for small values of h and t and that $u = h^2/t^3$. In LH83, Fig. 1, it is observed that t decreases as h decreases for small values leading to an increase of u for small h and t due to the stronger dependence of u on t than on h. However, for realistic physical situations at sea the larger values of h is of primary interest, for which $E[u \mid h]$ increases as h increases.

The expected value of u is given by

$$E[u] = E\left[\frac{h^2}{t^3}\right] = \int_0^\infty \int_0^\infty \frac{h^2}{t^3} p(h,t) dh dt = \int_0^\infty \int_0^\infty u\, p(h,u) dh du \tag{22}$$

Fig. 4 shows $E[u]$ versus ν in the range 0.1 to 0.6, and a quadratic increase of $E[u]$ with ν is clearly seen ranging from about 1 to 1.7 for these ν values.

4. STOKES TRANSPORT

Statistical properties of the non-dimensional Stokes transport m (from which the statistical properties of the Stokes transport M can be obtained) can be derived by using the LH83 *pdfs* in Eqs. (6) and (13). First, the joint *pdf* of m and h is obtained from Eq. (6) by a change of variables from (h,t) to (h,m). This transformation only affects t versus m, i.e. $t = h^2 m^{-1}$ according to Eq. (17), yielding the Jacobian $|\partial t / \partial m| = h^2 / m^2$; corresponding to a one-to-one transformation since t decreases monotonically as m increases. Consequently the result is

$$p(h,m) = C \cdot \exp\left\{-h^2\left[1+\frac{1}{\nu^2}(1-\frac{m}{h^2})^2\right]\right\} \quad (23)$$

Similarly, the conditional *pdf* of m given h is obtained from Eq. (13) by a change of variables from (h,t) to (h,m), yielding (by using the Jacobian $|\partial t/\partial m|$)

$$p(m\,|\,h) = \frac{2}{\sqrt{\pi}\nu(1+erf(h/\nu))}\frac{1}{h}\exp\left[-\frac{h^2}{\nu^2}(1-\frac{m}{h^2})^2\right] \quad (24)$$

It should be noted that the Jacobian is zero for $h = 0$ and has a singularity for $m = 0$. However, this does not affect the *pdfs* in Eqs. (23) and (24) as they are well defined.

Fig. 5 shows the isocontours of $p(h,m)$ for $\nu = 0.354$ (i.e. corresponding to the example given in Section 5), and the quadratic increase of m with h (Eq. (17)) is clearly seen. The peak value of the *pdf* is $p_{max} = 3.3$ and is located at $h = 5.4 \cdot 10^{-5}$ and $m = 2.9 \cdot 10^{-9}$, i.e. at very low values of h and m as seen in Fig. 5 (but this *pdf* has no singularity).

Fig. 6 shows the *pdf* of m for $\nu = 0.1, 0.6$ and is based on integration of the joint *pdf* in Eq. (23) (and in Fig. 5). It appears that the *pdf* of m is slightly less sensitive to the value of ν than $p(u)$ shown in Fig. 2.

Fig. 7 shows the expected value of m given h for $\nu = 0.1, 0.6$

$$E[m\,|\,h] = \int_0^\infty m\, p(m\,|\,h)dm \quad (25)$$

where $p(m\,|\,h)$ is given in Eq. (24). It appears that $E[m\,|\,h]$ increases as h increases reflecting the features of $p(h,m)$ shown in Fig. 5, and that the results are almost insensitive to a change in ν.

The expected value of m is given by

$$E[m] = E\left[\frac{h^2}{t}\right] = \int_0^\infty\int_0^\infty \frac{h^2}{t} p(h,t)dhdt$$
$$= \int_0^\infty\int_0^\infty m\, p(h,m)dhdm \tag{26}$$

Fig.8 shows $E[m]$ versus ν in the range of 0.1 to 0.6, and a quadratic increase of $E[m]$ with ν is clearly seen ranging from about 1 to 1.08 for these ν values.

5. EXAMPLE OF RESULTS

An example is included to illustrate the application of the results for practical purposes using data typical for field conditions. A Phillips spectrum is chosen as the deep water wave spectrum (see Tucker and Pitt (2001))

$$S(\omega) = \alpha \frac{g^2}{\omega^5} \; ; \; \omega \geq \omega_p = \frac{g}{U_{10}} \tag{27}$$

where $\alpha = 0.0081$ is the Phillips constant, ω_p is the spectral peak frequency, and U_{10} is the mean wind speed at the 10 m elevation. Be using the definition of the spectral moments in Eq. (11) it follows that

$$m_0 = \alpha \frac{U_{10}^4}{4g^2} \tag{28}$$

$$m_1 = \alpha \frac{U_{10}^3}{3g} \tag{29}$$

$$m_2 = \alpha \frac{U_{10}^2}{2} \tag{30}$$

which gives the bandwidth parameter in Eq. (10)

$$\nu^2 = 0.125 \, , \nu = 0.354 \tag{31}$$

for which the joint *pdfs* of (h, u) and (h, m) are plotted in Figs. 1 and 5, respectively. Thus, for this particular wave spectrum the integrals in Eqs. (22) and (26) can be integrated numerically giving, respectively,

$$E[u] = 1.226 \tag{32}$$

$$E[m] = 1.030 \tag{33}$$

By choosing a wind speed of $U_{10} = 10.4\,\text{m/s}$ (i.e. corresponding to a significant wave height of $H_s = 4\sqrt{m_0} = 2\sqrt{\alpha}/(g/U_{10}^2) = 2.0\,\text{m}$ and a spectral peak period of $T_p = 2\pi/\omega_p = 2\pi/(g/U_{10}) = 6.7$ s) it follows that

$$U_{char} = 0.10\,\text{m/s} \quad (\text{Eq. (13)}) \tag{34}$$

$$M_{char}/\rho = 0.310\,\text{m}^2/\text{s} \quad (\text{Eq. (15)}) \tag{35}$$

Thus, the mean surface Stokes drift velocity and the mean Stokes transport are obtained as

$$E[U_s] = U_{char}E[u] = 0.10 \cdot 1.226\,\text{m/s} = 0.123\,\text{m/s} \tag{36}$$

$$E[M/\rho] = (M_{char}/\rho)E[m] = 0.310 \cdot 1.030\,\text{m}^2/\text{s} = 0.319\,\text{m}^2/\text{s} \tag{37}$$

It appears that the ratio between the surface Stokes drift velocity and the wind speed at the 10m elevation ($E[U_s]/U_{10}$) is 1.2 percent. Thus, this example gives a result which overall is consistent with those obtained by Rascle et al. (2008, Fig. 8), who found that the surface Stokes drift parameter for the sea state $\bar{U}_s = \pi^3 H_s^2/(gT_3^3)$ (where $T_3 = 2\pi(m_0/m_3)^{1/3}$) is in the range of 0.8 to 1.6% of U_{10} in the open sea. However, it should be noted that the results are not directly comparable since the present results are valid for the mean of the surface Stokes drift for individual waves in the sea state, while the Rascle et al. (2008) results are valid for the surface Stokes drift parameter for the sea state.

The present results are valid for long-crested (2D) waves. Rascle and Ardhuin (2013) found that for short-crested (3D) waves the values of $\bar{U}_s$ for 2D waves were reduced by 20 percent when the directional spreading is taken into account. It should be noted that a very similar reduction in the surface Stokes drift was also suggested in Webb and Fox-Kemper (2011, Appendix 4). Moreover, the effects of directional spreading and multidirectional waves have been further explored by Webb (2013, Ch. 2), suggesting that more interesting effects occur when swell and wind waves coexist with different directional properties. Thus, by reducing the present example value for 2D waves by 20 percent $E[U_s]/U_{10}$ is 1 percent, which is consistent (but not directly comparable) with that obtained by Rascle and Ardhuin (2013, Fig. 6a); for 3D waves they found that the surface Stokes drift is approximately 1 percent of $U_{10} = 10.4\,\text{m/s}$ for $H_s = 2\,\text{m}$.

It should be noted that a commonly used procedure for random waves would be to use Eqs. (1) and (2) and substitute for an equivalent sinusoidal wave. This is obtained by replacing T with T_p and H with H_{rms} (i.e. the root-mean-square (*rms*) wave height which is $H_{rms} = H_s / \sqrt{2}$ for a narrow-band process when H is Rayleigh-distributed). Thus, substitution of $H_{rms} = \sqrt{2}$ m and $T_p = 6.7$ s in Eqs. (4) and (5) gives

$$U_s = 0.042\,\text{m/s}$$

$$M / \rho = 0.23\,\text{m}^2\text{/s}$$

It appears that these values are smaller than those obtained in Eqs. (36) and (37), respectively. In particular this value of U_s is substantially smaller than that in Eq. (36), and hence the present method should be used to estimate the Stokes drift for random waves.

For the application of the present results it should be noted that, except for swell without wind, the Stokes drift is associated with current generated by surface wind, and that this current decays with the depth below the surface.

6. SUMMARY

A simple analytical method which can be used to give estimates of the Stokes drift based on statistics of short-term observations of wave conditions is provided. This is achieved by providing bivariate distributions of H with surface Stokes drift as well as with volume Stokes transport. These bivariate distributions are obtained by transformations of a joint distribution of (H,T), by using the joint *pdf* model of H and T given by Longuet-Higgins (1983). The statistical properties of these Stokes drift parameters are discussed. An example of results corresponding to typical field conditions are also presented, giving consistent results with those obtained by Rascle and Ardhuin (2013) based on wave hindcast of the wave parameters.

ACKNOWLEDGEMENT

This work was carried out as part of the project "Air-Sea Interaction and Transport Mechanisms in the Ocean" funded by the Norwegian Research Council. This support is gratefully acknowledged. Professor Bernt J. Leira at the Department of Marine Technology, NTNU is also gratefully acknowledged for valuable discussions.

REFERENCES

Cavanié, A., Arhan, M., Ezraty, R.A. (1976). A statistical relationship between indivdual heights and periods of storm waves. In *Proc. Conf. on Behaviour of Offshore Structures*, Vol. II, p. 354-360.

Dean, R.G., Dalrymple, R.A. (1984). Water Wave Mechanics for Engineers and Scientists. Prentice-Hall, Inc., New Jersey, USA.

Lindgren, G., Rychlik, L. (1982). Wave characteristic distributions for Gaussian waves – wave length, amplitude and steepness. *Ocean Engng* 9; 411-432.

Longuet-Higgins, M.S. (1983). On the joint distribution of wave periods and amplitudes in a random wave field. *Proc. Roy. Soc. London*, Ser. A, 389; 241-258.

Losada, M.A., Giminez-Curto, L.A. (1981). Flow characteristics on rough, permeable slopes under wave action. *Coastal Eng*, 4; 187-206.

Myrhaug, D. (2013). Some statistical aspects of wave-induced drift in sea states. *Coastal Eng*, 78; 53-56.

Myrhaug, D. Stokes drift estimation based on long-term variation of wave conditions. *Proc IMechE Part M. J Engineering for the Maritime Environment*, doi:

10.1177/1475090213506699, in press.

Myrhaug, D., Holmedal, L.E. (2005). Bottom friction caused by boundary layer streaming beneath random waves for laminar and smooth turbulent flow. *Ocean Engng*, 32; 195-222.

Myrhaug, D., Holmedal, L.E., Rue, H. (2004). Bottom friction and bedload sediment transport caused by boundary layer streaming beneath random waves. *Appl. Ocean Res.*, 26; 183-197.

Myrhaug, D., Kjeldsen, S.P. (1984). Parametric modelling of joint probability density distributions for steepness and asymmetry in deep water waves. *Appl. Ocean Res.*, 6; 207-220.

Myrhaug, D., Kvålsvold, J. (1995). Comparative study of joint distributions of primary wave characteristics. *J. Offshore Mech. and Arctic Engng*, 117; 91-98.

Myrhaug, D., Ong, M.C., Føien, H., Gjengedal, C., Leira B.J. (2009). Scour below pipelines and around vertical piles due to second-order random waves plus a current. *Ocean Engng*, 36 (8); 605-616.

Rascle, N., Ardhuin, F. (2013). A global wave parameter database for geophysical applications. Part 2: Model validation with improved source term parameterization. *Ocean Modelling*, 70; 174-188.

Rascle, N., Ardhuin, F., Queffeulou, P., Croizé-Fillon, D. (2008). A global wave parameter database for geophysical applications. Part 1: Wave-current-turbulence interaction parameters for the open ocean based on traditional parameterizations. *Ocean Modelling*, 25; 154-171.

Srokosz, M.A., Challenor, P.G. (1987). Joint distribution of wave height and period: A critical comparison. *Ocean Engng*, 14;295-311.

Stansell, P., Wolfram, J., Linfoot, B. (2004). Improved joint probability distribution for ocean wave heights and periods. *J. Fluid Mech.*, 503; 273-297.

Tucker, M. J., Pitt, E.G. (2001). *Waves in Ocean Engineering*. Elsevier, Amsterdam.

Webb, A. A. (2013). Stokes drift and meshless wave modeling. PhD Thesis, Faculty of the Graduate School, University of Colorado. http://www.geo.brown.edu/research/Fox-Kemper/pubs/pdfs/WebbThesis.pdf

Webb, A., Fox-Kemper, B. (2011). Wave spectral moments and Stokes drift estimation. *Ocean Modelling*, 40; 273-288.

Figure captions

Fig. 1 Isocontours of $p(h,u)$ for $\nu = 0.354$. The difference between each level of the contours is 0.1.

Fig. 2 $p(u)$ versus u for $\nu = 0.1, 0.2, 0.3, 0.4, 0.5, 0.6$.

Fig. 3 $E[u\,|\,h]$ versus h for $\nu = 0.1, 0.2, 0.3, 0.4, 0.5, 0.6$.

Fig. 4 $E[u]$ versus ν.

Fig. 5 Isocontours of $p(h,m)$ for $\nu = 0.354$. The difference between each level of the contours is 0.15.

Fig. 6 $p(m)$ versus m for $\nu = 0.1, 0.6$.

Fig. 7 $E[m\,|\,h]$ versus h for $\nu = 0.1, 0.6$.

Fig. 8 $E[m]$ versus ν.

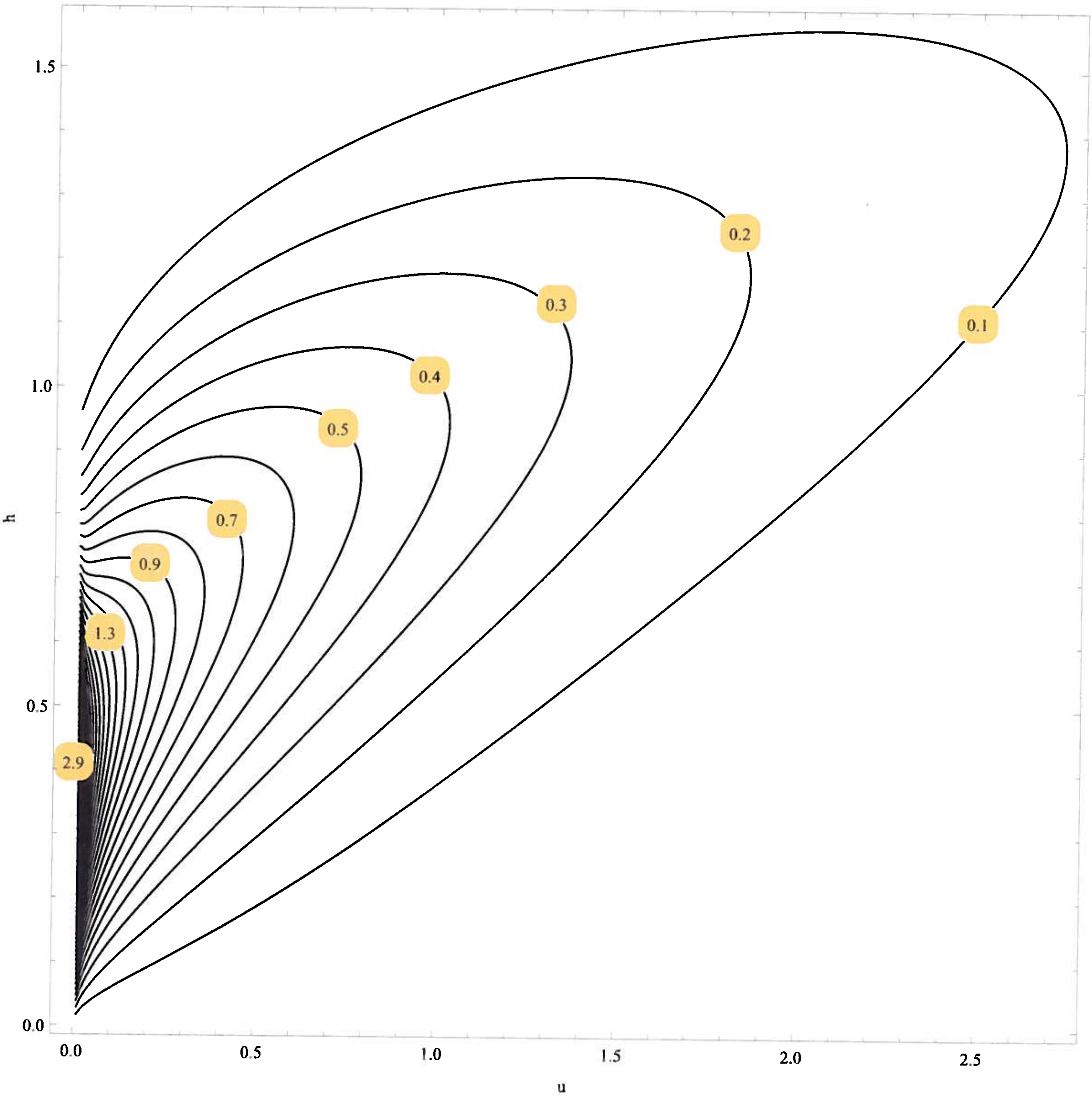
0.1
0.2
0.3
0.4
0.5
0.7
0.9
1.3
2.9
1.5
1.0
0.5
0.0
h
0.0
0.5
1.0
1.5
2.0
2.5
u

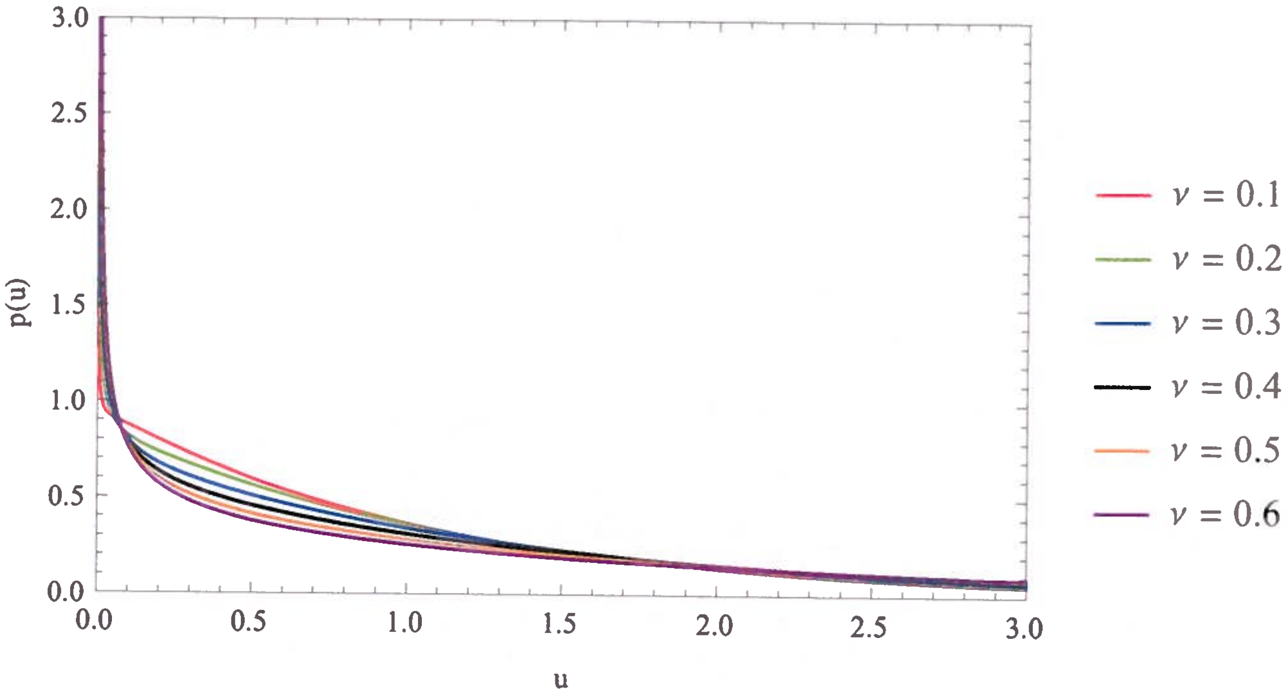
p(u)
3.0
2.5
2.0
1.5
1.0
0.5
0.0
0.5
1.0
1.5
2.0
2.5
3.0
u
ν = 0.1
ν = 0.2
ν = 0.3
ν = 0.4
ν = 0.5
ν = 0.6

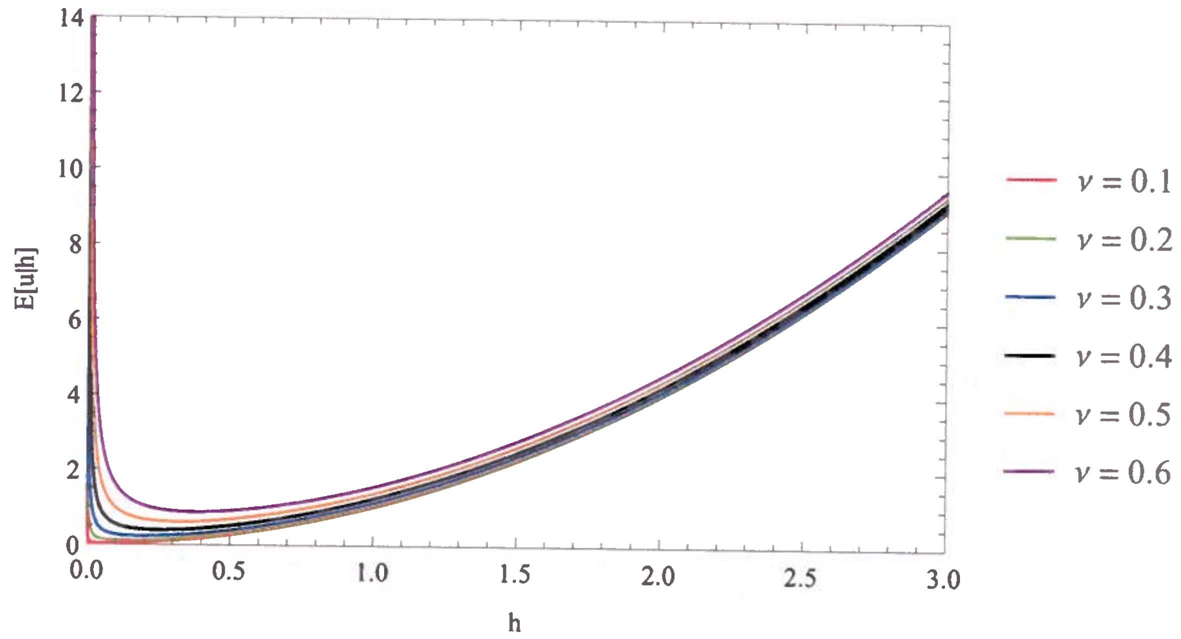
14
12
10
8
6
4
2
0
E[u|h]
0.0
0.5
1.0
1.5
2.0
2.5
3.0
h
ν = 0.1
ν = 0.2
ν = 0.3
ν = 0.4
ν = 0.5
ν = 0.6

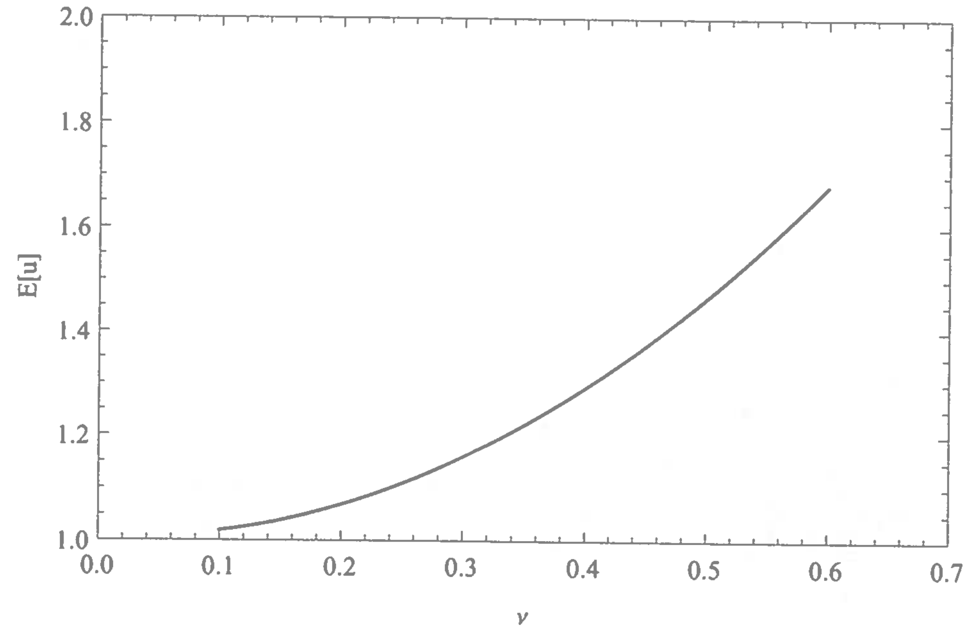
E[u]
2.0
1.8
1.6
1.4
1.2
1.0
0.0
0.1
0.2
0.3
0.4
0.5
0.6
0.7
ν

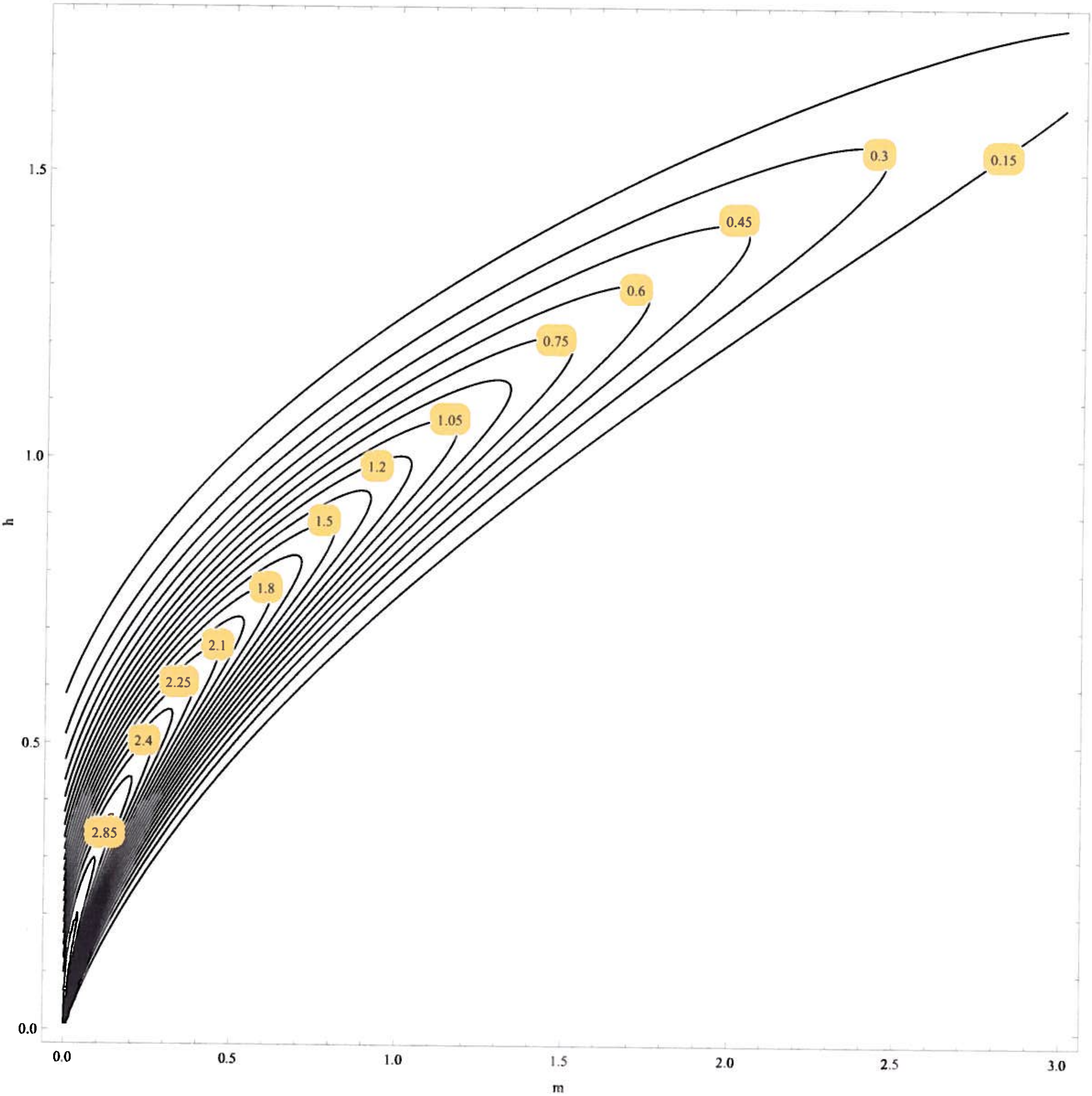

0.3
0.15
0.45
0.6
0.75
1.05
1.2
1.5
1.8
2.1
2.25
2.4
2.85
1.5
1.0
0.5
0.0
h
0.0
0.5
1.0
1.5
2.0
2.5
3.0
m

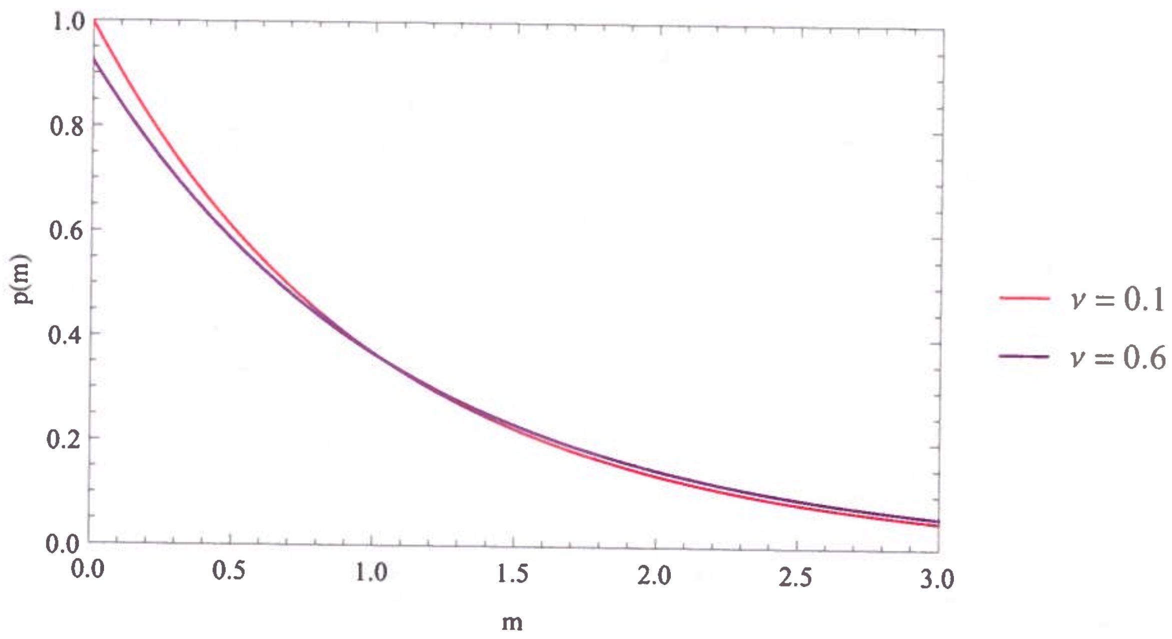

1.0
0.8
0.6
0.4
0.2
0.0
p(m)
0.0
0.5
1.0
1.5
2.0
2.5
3.0
m
ν = 0.1
ν = 0.6

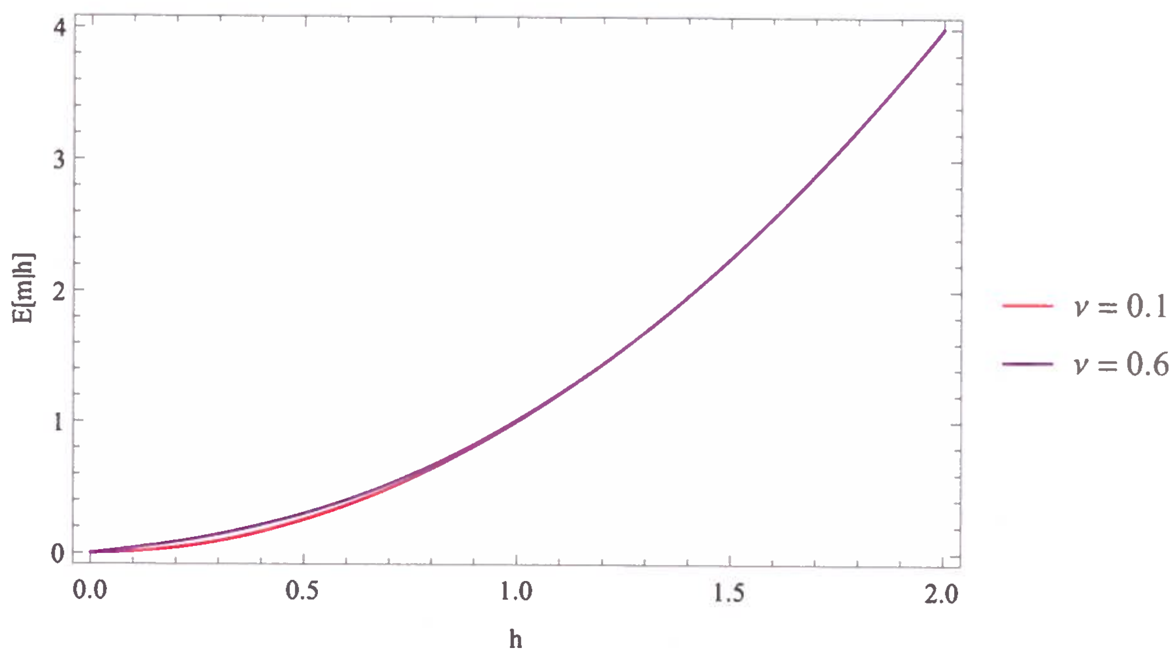
E[m|h]
4
3
2
1
0
0.0
0.5
1.0
1.5
2.0
h
ν = 0.1
ν = 0.6

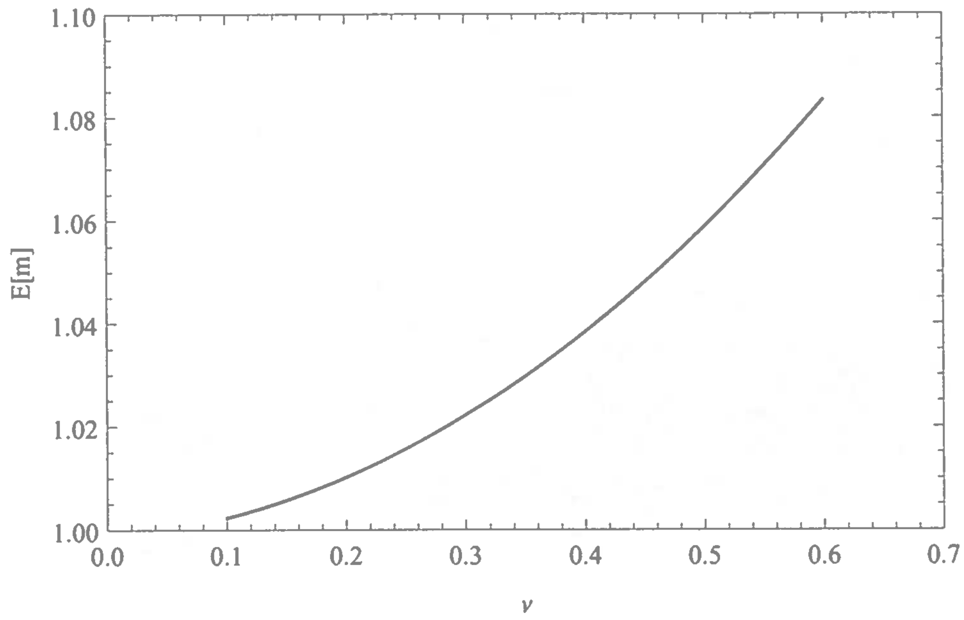
1.10
1.08
1.06
1.04
1.02
1.00
E[m]
0.0
0.1
0.2
0.3
0.4
0.5
0.6
0.7
ν